Electromagnetic Interference Shielding Effectiveness of Composites Based on Polyurethane Derived From Castor Oil and Nanostructured Carbon Fillers

Claudia Merlini ⬡,[1,2] Alessandro Pegoretti,[3] Patricia Cristine Vargas,[1] Tairan F. da Cunha,[1]
Sílvia D.A.S. Ramôa,[1] Bluma G. Soares,[4] Guilherme M. O. Barra[1]
[1]Departament of Mechanical Engineering, Universidade Federal de Santa Catarina (UFSC), Florianópolis, Santa Catarina, Brazil

[2]Departament of Engineering, Universidade Federal de Santa Catarina (UFSC), Blumenau, Santa Catarina, Brazil

[3]Department of Industrial Engineering, University of Trento, Trento, 38123, Italy

[4]Departament of Metallurgical and Materials Engineering, Universidade Federal do Rio de Janeiro (UFRJ), Rio de Janeiro, Brazil

Graphene nanoplatelets (xGnP), expanded graphite (EG), multiwall carbon nanotubes (MWCNTs), and carbon black (CB) were dispersed in various amounts in a thermosetting polyurethane (PU) matrix derived from castor oil and composite plaques were obtained by compression molding. The electrical percolation threshold was found to be 0.1 vol% for MWCNT, 0.5 vol% for xGnP, 2.8 vol% for CB, and 2.7 vol% for EG-filled systems. The relation between electrical conductivity, morphology, and electromagnetic interference shielding effectiveness (EMI SE) of the resulting composites was studied to understand how the EMI SE is influenced by morphology and electrical conductivity of each filler. The composites display significantly distinct EMI SE values, depending on the type of carbon filler and its volume fraction. Composite based in PU/EG and PU/xGnP exhibited the highest EMI SE values (70 and 47 −dB, respectively); however, PU/MWCNT composites showed higher EMI SE (24 −dB) value at the same filler content (3 vol%) than the other composite system. POLYM. COMPOS., 40:E78–E87, 2019. © 2017 Society of Plastics Engineers

INTRODUCTION

Over the last decades, interest in developing carbonaceous filled polymer composites has increased significantly due to the possibility to produce new materials with high flexibility, environmental resistance, cost effectiveness, and easy processing, which are important for electromagnetic shielding applications [1–4]. Usually, these conductive composites can overcome the drawbacks presented by conventional metal-based EMI shielding materials, allowing the development of lightweight structures [5]. Carbon black (CB) and carbon fibers (CF) were first investigated as carbonaceous fillers, but recently carbon nanotubes (CNT), graphene, and expanded graphite nanoplatelets have received intensive consideration for EMI shielding application [1, 6]. The electromagnetic interference shielding effectiveness (EMI SE) and electrical conductivity of these nanocomposites depend of a wide variety of parameters, including the structure, properties, and interactions of both components (polymer matrix and filler) [1, 7–9].

Designing efficient EMI materials also requires to overcome difficulties in the processing of polymer composites filled with carbonaceous particles, especially those related to the dispersion and distribution of the filler into the polymeric matrix. A major challenge in developing composites filled with graphite or expanded graphite (EG) is the separation of the layered sheets (exfoliation) to achieve higher electrical conductivity and EMI SE values at lower conductive filler content [10]. Also the dispersion of graphene

TABLE 1. Typical properties of carbonaceous fillers used in this work.

Fillers	Manufacturer	Commercial name	Carbon purity (%)	Surface area ($m^2 \, g^{-1}$)	Density ($g \, cm^{-3}$)	Electrical conductivity ($S \, cm^{-1}$)[b]
Graphene nanoplatelets	XG Sciences	xGnP® Grade M	>99.5	120–150	2.05[a]	$(6.9 \pm 0.4) \times 10^2$
Graphite	Nacional de Grafite Ltda	Micrograf HC 30	>99.7	26	1.80 [13]	$(3.4 \pm 0.4) \times 10^2$
Carbon black	Cabot	VULCAN® XC-72	>98	254 [21]	1.93 [22]	$(7.2 \pm 0.1) \times 10^{-1}$
Multiwall carbon nanotubes	Nanocyl S.A	Nanocyl™ NC7000	>90	250–300	2.15[a]	$(1.3 \pm 0.1) \times 10^1$

[a]Private communication from mr. Sithiprumnea Dul.
[b]Measured by four-probe standard method.

nanoplatelets and carbon nanotubes can significantly improve the EMI SE, electrical conductivity, mechanical properties, and processability of composite [10, 11].

Considering that several factors can affect the EMI SE when carbon fillers are incorporated into polymeric matrices, it is important to know their structure and intrinsically properties to understand the way by which the filler affects the final properties of nanocomposite. Usually, depending on the type and amount of the carbon filler incorporated into insulating polymer matrix, different values of electrical conductivity and EMI SE can be achieved. This behavior is mainly related to the aspect ratio of the carbonaceous filler [12] and its ability to form a conductive network in the matrix. Kuester, Merlini, Barra, Ferreira Jr, Lucas, de Souza, and Soares [13] have reported for SEBS/EG composites a maximum EMI SE of −11.69 dB (∼93% of attenuation) by using 20 wt% (∼13 vol%) of EG [13]. Liang, Wang, Huang, Ma, Liu, Cai, Zhang, Gao, and Chen [14] have reported that 15 wt% (i.e., ∼8 vol%) of graphene was necessary to achieve an EMI SE of −21 dB for graphene/epoxy composites. In a recent review [1] is reported that composites based on CB usually display poor EMI SE performance, for which very high CB amount (>25 wt% or 15 vol%) or elevated thickness (>2 mm) is necessary to achieve EMI value of −20 dB. On the other hand, due to its cylindrical structure, CNT [15, 16] provides high aspect ratio, that allows the development of composites with higher electrical conductivity and EMI SE at lower filler content [6, 17]. Al-Saleh, Saadeh, and Sundararaj [18] reported a comparative study of acrylonitrile butadiene styrene (ABS) nanocomposites containing multiwall carbon nanotubes (MWCNTs), carbon fibers (CF), and CB. The authors reported that the EMI SE and electrical conductivity of nanocomposites containing 15 wt% of MWCNT, CNF, and CB decrease in the following order: MWCNT > CNF > CB, whose EMI SE values were −50, −35, and −20 dB, respectively.

Several studies have been reported on the development of nanocomposites based on different carbon fillers for shielding applications [3, 5, 6, 12–14, 17–19]. However, the measurements are usually performed at various frequencies and samples thickness, which makes difficult a direct comparison of their performance [1].

Considering this framework, the aim of this study is to understand the effect of various nanostructured carbon filler incorporated into a thermosetting polyurethane (PU) derived from castor oil on the electrical conductivity and EMI SE. PU is an interesting polymeric matrix to produce conductive polymer nanocomposites for EMI SE applications because it can be derived from renewable sources and displays versatile feature of molding [20, 23], which not require the use of solvent and high process temperatures.

EXPERIMENTAL

Materials

The PU derived from castor oil (PU) (IMPERVEG® UG 132 A) used in this study was supplied by the company IMPERVEG® *Comércio e Prestações de Serviço Ltda,* as two components: a polyol derived from castor oil (a trifunctional polyester) and a prepolymer, with 3% of the free isocyanate, which was synthesized by reacting diphenylmethanediisocyanate (MDI) with the polyol. The specifications, most of them provided by the manufacturers, of the carbonaceous fillers used in this work and their typical properties are present on Table 1.

Preparation of Composites

The composites were prepared by compression molding, where first the polyol and prepolymer (mass ratio of 2/1) were mechanically mixed under vacuum for 5 min. Then, a certain weight fraction of carbonaceous fillers was incorporated to this mixture and stirred under vacuum for 5 min. The resulting composite was poured into a metallic mold, maintained for 2 h at room temperature, and then subjected to compression molding at 10.7 MPa for 4 h. Composites of polyurethane with graphene nanoplatelets (xGnP), expanded graphite (EG), carbon black (CB), and MWCNTs were prepared with different fillers content. For each system, volume fractions of fillers as high as possible were incorporated, being that, above these values, the viscosity of the system prevented the molding of composites.

Characterization

Electrical conductivity measurements of fillers and high-conductivity composites were performed according to ASTM F42–93, using the four-probe standard method with a Keithley 6,220 current source to apply the current and a Keithley Model 6517A electrometer to measure the potential difference. The measurements on composites were performed on rectangular specimens, with a width of 15 mm and a length of 30 mm. The fillers were compacted using a hydraulic press, at pressures up to 3 MPa on cylindrical specimens with 25 mm in diameter. The electrical conductivity of neat PU and low-conductivity composites were performed according to ASTM D-257, on circular specimens of 90 mm of diameter, using a Keithley 6517A electrometer connected to a Keithley 8009 test fixture.

Micrographs of cryogenically fractured samples were obtained using a field emission scanning electron microscope (FESEM), Jeol JSM – 6701F. The fracture surfaces were coated with gold and then observed at an accelerating voltage of 5 kV.

The morphology of carbonaceous fillers and their dispersion in the PU matrix were investigated by transmission electron microscopy (TEM). The fillers were dispersed in isopropyl alcohol and then were placed on a grid of cooper 300 mesh covered by amorphous carbon. Ultrathin slices (~80 nm in thickness) of the composites were cut by an ultramicrotome (RMC Boeckeler) equipped with diamond knife and then deposited on a 200 mesh copper grid. All the TEM micrographs were collected with a Jeol JEM-1100 microscope operating an accelerating voltage of 100 kV.

EMI SE characterization in the X-band frequency range (8.2–12.4 GHz) were performed with an Agilent Technology PNA series network analyzer (N5230C Agilent PNA-L, Santa Clara, CA) and a standard rectangular waveguide. Rectangular specimens (width 10 mm, length 23 mm, and thickness 2 mm) were placed between the two sections of the waveguide. EMI SE, reflected energy (SE_R), transmitted energy (SE_T), and absorbed energy (SE_A) were calculated from complex scattering parameters that correspond to reflection ($S*_{11}$) and transmission (S^*_{21}).

RESULTS AND DISCUSSION

The electrical conductivity as a function of carbonaceous filler type and content is showed in Fig. 1. As expected, all composites exhibited an increase in the electrical conductivity as the amount of conductive filler increases. However, it can be noticed that the electrical conductivity is dependent on the filler type. This behavior can be mainly attributed to the morphology and aspect ratio of each filler that contributes differently to the formation of electrically conducting pathways [1, 18]. Similar behavior was reported by Al-Saleh et al. [18],
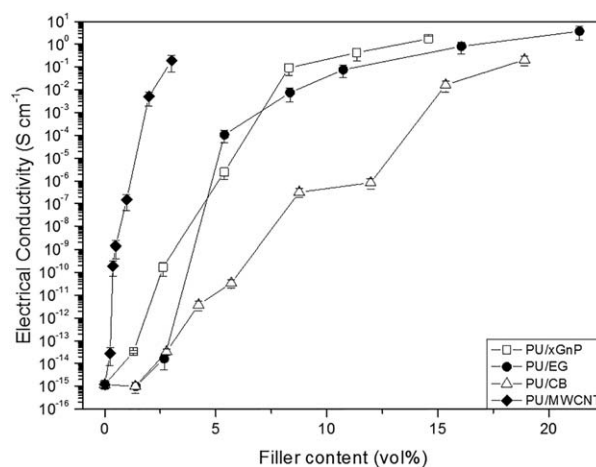
FIG. 1. Electrical conductivity as a function of fillers content for composites containing different carbonaceous fillers.

who studied nanocomposites of acrylonitrile–butadiene-styrene (ABS) with different carbon nanofillers (CB, carbon nanofiber (CNF), and CNT). In those systems, the increase in the electrical conductivity of the nanocomposites with the same nanofiller loading is related to the aspect ratio of the fillers, wherein high aspect ratio facilitates the formation of a conductive network at lower filler content.

The data presented in Fig. 1 were fitted with the scaling law of percolation theory [20] to obtain the percolation threshold, that is, the critical concentration of conducting filler required to form a conductive network in the polymer matrix [18]. It is important to highlight that when the percolation theory is used, it is assumed that the conductive particles are statistically evenly distributed within the matrix. Therefore, deviations of the experimental results from those predicted by the percolation theory can be found [26]. The percolation threshold and critical exponent values of each polymer composites are summarized in Table 2. The percolation threshold for PU/xGnP, PU/EG, PU/CB, and PU/MWCNT resulted to be 0.5, 2.7, 2.8, and 0.1 vol%, respectively. The TEM pictures of Fig. 2 indicate that the carbonaceous fillers display different morphologies, such as particles (CB), layered sheets (EG), nanoplatelets (xGnP), and fibrous (MWCNT) [24], resulting in different aspect ratio and surface area (as shown previously in Table 1). These morphological features have an influence on the electrical conductivity values and percolation threshold. In fact, PU/MWCNT composite presents the lowest electrical percolation threshold due to the high aspect ratio of MWCNT (~158), which facilitates the conductive network formation in PU matrix at very low filler content (0.1 vol%). At 0.5 vol%, the PU/MWCNT composites exhibits approximately a 10^6-fold increase in the electrical conductivity (1.4×10^{-9} S cm^{-1}) when compared to pure PU (1.2×10^{-15} S cm^{-1}). On the other hand, at the same loading, the xGnP-, EG-, and CB-based composites display the same electrical conductivity level of neat PU

TABLE 2. Percolation threshold and critical exponent for different PU/carbonaceous fillers systems.

System	Percolation threshold (f p(vol%))	Critical exponent (t)	Linear correlation coefficient (R)
PU/xGnP	0.5	12.1	0.98
PU/EG	2.7	4.9	0.99
PU/CB	2.8	10.8	0.91
PU/MWCNT	0.1	8.5	0.98

matrix. PU/xGnP composites also display low percolation threshold (0.5 vol%), as the structure of few layer graphene provides high aspect ratio and surface area and improved contact between the filler. On the other hand, PU/CB composite exhibited higher percolation threshold (2.8 vol%) when compared to PU/MWCNT and PU/xGnP systems due to its low aspect ratio. PU/EG composite displays also higher percolation threshold (2.7 vol%) due to the stacked layers, which need to be exfoliated to improve more significantly the electrical conductivity of composite.

The critical exponent (t) of all composite systems studied in this work and reported in Table 2 are significantly higher than the values predicted by the classical theory for tridimensional systems which range from 2 to 4 [25]. This behavior can be associated to the fact that the theory does not take into consideration some specific features of the investigated conductive fillers, such as shape, particle size, and aspect ratio [13]. Usually, larger critical exponent have been associated with an electron hoping mechanism [13].

The influence of the conductive filler content on the microstructure of the PU/xGnP, PU/EG, PU/CB, and PU/MWCNT composites are showed in the FESEM micrographs presented in Fig. 3. The microstructure of cryogenically fractured surface of PU/xGnP composites reveals a very irregular fracture surface probably due to the breakage or pull-out of graphene sheets. As shown in Fig. 3 (a,b), xGnP particles are well dispersed in the matrix while EG agglomerates (Fig. 3(c,d)). FESEM images of PU/EG composites indicate the presence of stacked layers of EG, probably due to the low shear rate of the manual manufacturing process, which is not enough to exfoliate the filler. The PU/CB micrographs reveals that the CB particles tend to form small agglomerates that are well distributed into the PU matrix. Micrographs of PU/MWCNT containing 0.2 and 2 vol% of MWCNT shows that the carbon nanotubes are well dispersed and distributed into PU matrix thus inducing a conducting network.

The TEM micrograph of PU/xGnP composites containing 8.3 vol% of xGnP presented in Fig. 4a shows that the graphene nanoplatelets are well distributed and dispersed in the PU matrix, while EG agglomerates are observed
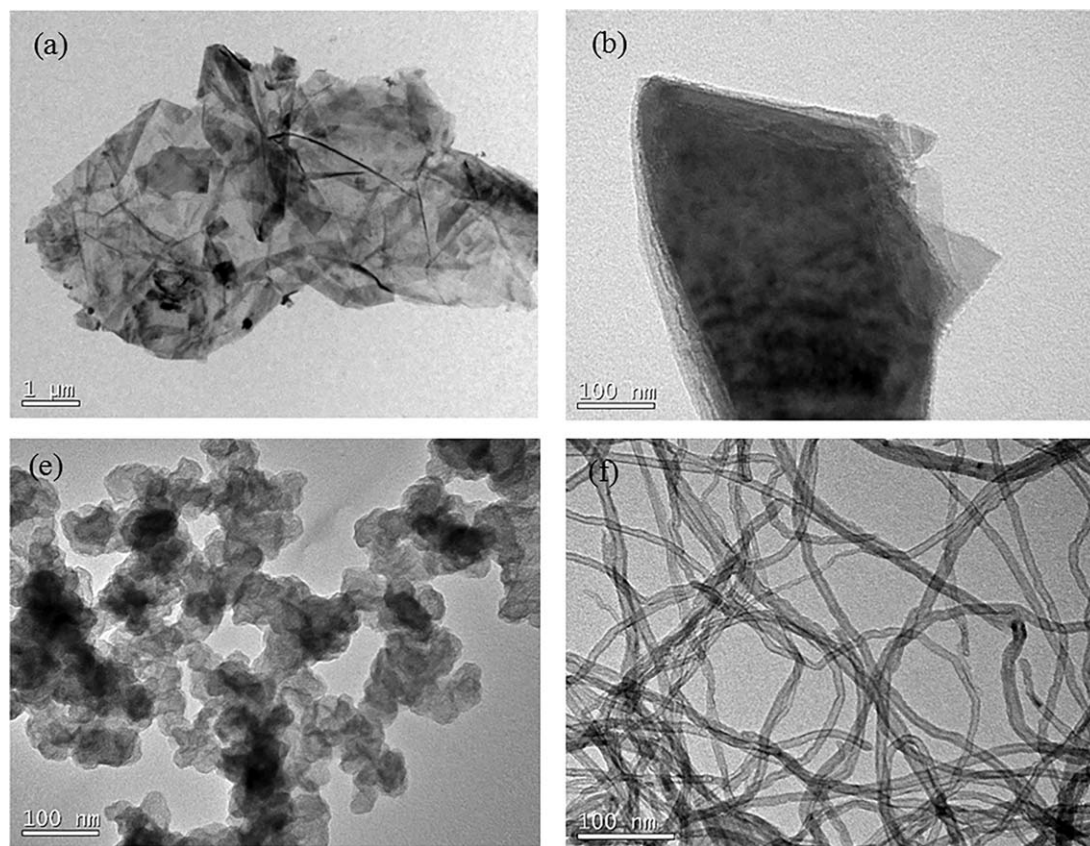
FIG. 2. TEM micrographs of (a) xGnP, (b) EG, (c) CB, and (d) MWCNT fillers.
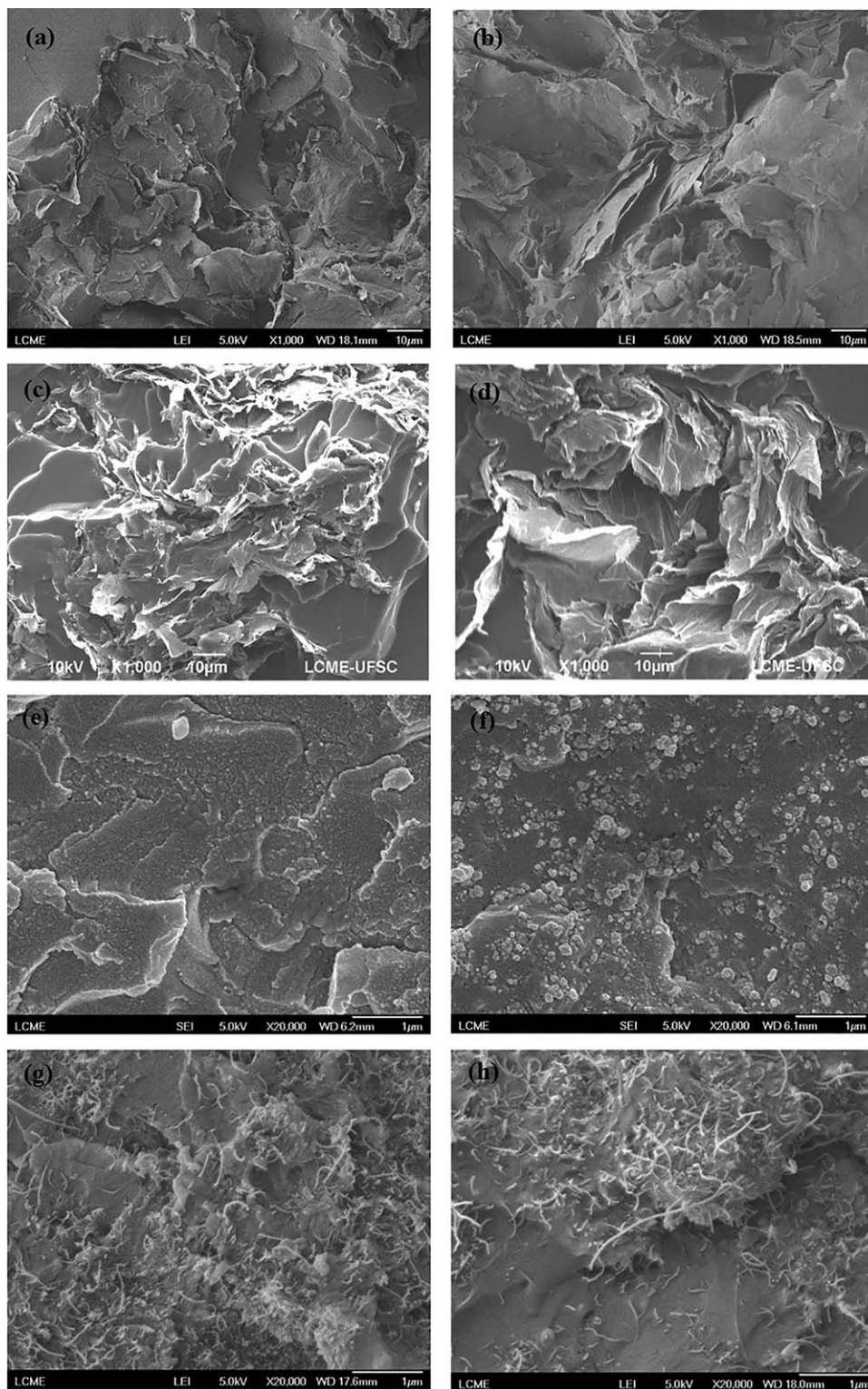
FIG. 3. FESEM micrographs of composites: (a) PU/xGnP_1.3 vol%, (b) PU/xGnP_5.4 vol%, (c) PU/EG_2.7 vol%, (d) PU/EG_5.4 vol%, (e) PU/CB_1.4 vol%, (f) PU/CB_5.7 vol%, (g) PU/MWCNT_0.2 vol%, and (h) PU/MWCNT_2.0 vol%.

for PU/EG composites (Fig. 4b). TEM micrograph of PU/CB containing 1.4 vol% of CB (Fig. 4c) shows CB agglomerates that are not well distributed in the PU. On the other hand, TEM micrograph of PU/MWCNT containing 0.5 vol% of

MWCNT (Fig. 4d) exhibits well-dispersed and distributed conducting phase in the PU matrix.

The EMI SE can be defined as the attenuation of electromagnetic waves performed by the shielding material
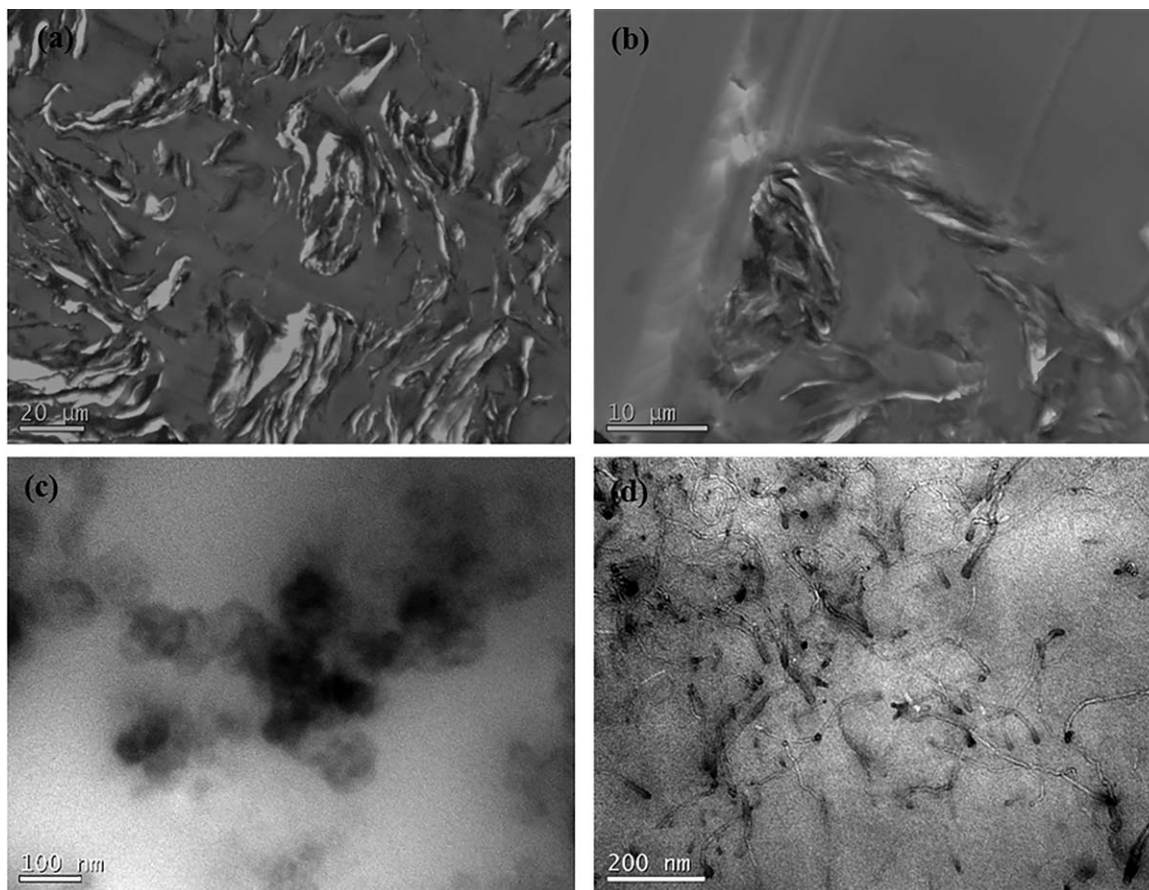
FIG. 4. TEM micrographs of composites: (a) PU/xGnP_8.3 vol%, (b) PU/EG_5.4 vol%, (c) PU/CB_1.4 vol%, and (d) PU/MWCNT_0.5 vol%.

[12]. The EMI SE of a material can be measured by the ratio between incident (I) to transmitted (T) power of electromagnetic waves, as defined in *Eq. 1* (in decibels (dB)) [13, 17, 20]:

$$\text{EMI SE (dB)} = 10 \log \frac{I}{T} \qquad (1)$$

Figure 5 shows the EMI SE of investigated composites as a function of volume fraction and type of carbonaceous filler over the frequency range of 8.2–12.4 GHz. First of all, it is possible to note that EMI SE of neat PU is practically null, indicating that the polymer is almost transparent to magnetic waves. For the composites with the same fillers, the increase in the filler content result in an improvement of EMI SE; however, this property is strongly dependent on the filler type. In fact, if we take into account the maximum EMI SE level, composites based on xGnP and EG present the highest SE, however, at higher filler content. The maximum EMI SE for PU/xGnP and PU/EG composites was around −70 and −76 dB for 14.6 and 21.4 vol% of conductive filler, respectively. At similar filler loading (18.9 vol%), PU/CB composites display a EMI SE of −29 dB that is significantly lower than those of PU/xGnP and PU/EG composites. This evidences the better performances of xGnP- and

EG-based composites as a shield material against electromagnetic interference. The lowest performance of PU/CB composites can be related to the lowest aspect ratio and electrical conductivity. Additionally, the tendency of CB particles to form agglomerates allows the existence of regions devoid of carbon black particles, where occurs the passage of radiation, reducing the EMI SE of overall composite [3].

On the other hand, if we consider the maximum EMI SE at the lowest filler content, PU/MWCNTs manifest superior EMI shielding performance. At a similar amount of conductive filler (~3 vol%), composites with MWCNT, xGnP, EG, and CB have shown EMI SE of about −24, −6, −5, and −4 dB, respectively, which confirms the best efficiency of carbon nanotubes. EMI SE is mainly related to electrical conductivity of composites, but also depends on the filler type and its size, shape, dispersion, and distribution into the matrix [6]. According to Thomassin, Jérôme, Pardoen, Bailly, Huynen, and Detrembleur [1], the highest SE is observed for carbon fillers with higher aspect ratio, due to the possibility to change more significantly the electrical conductivity. Based on this context, the superior performance of PU/MWCNT compared to PU/xGnP, PU/EG, and PU/CB can be attributed to the high number of interconnected
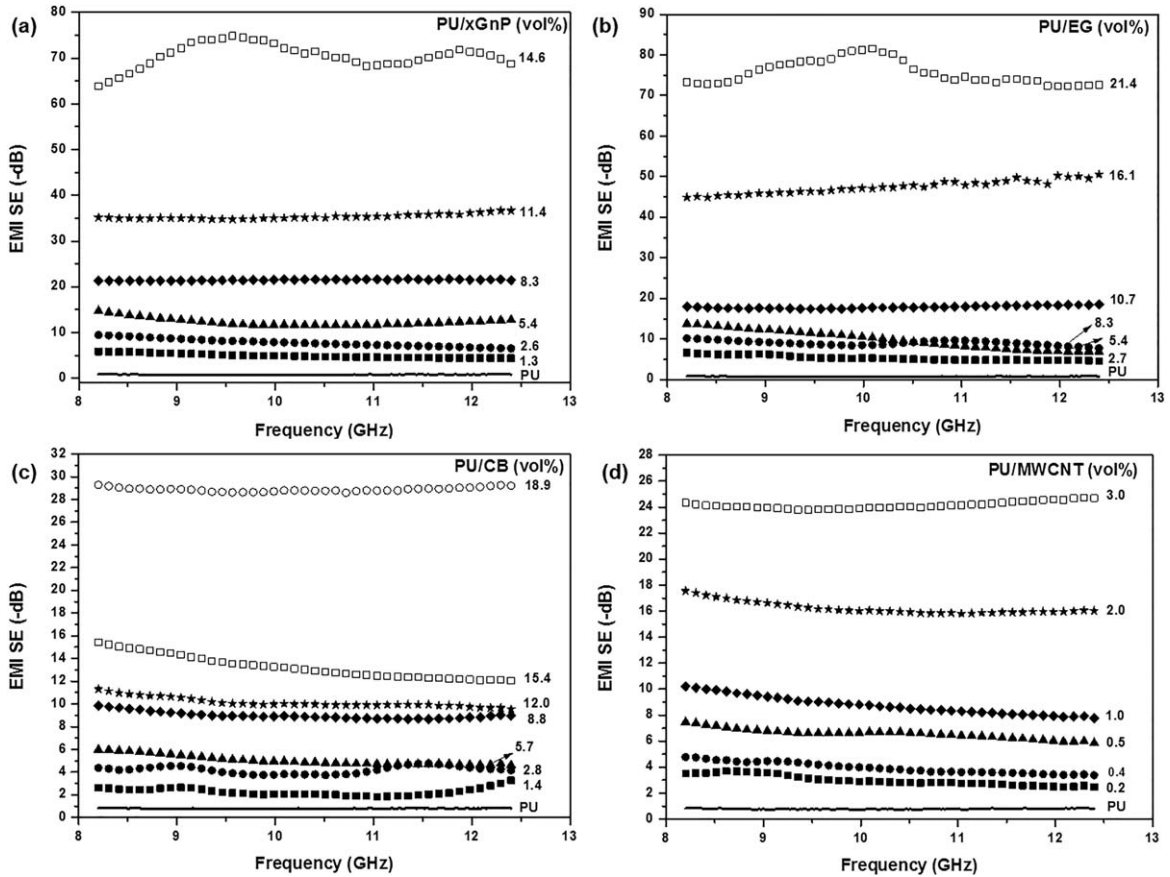
FIG. 5. EMI SE in the X-band frequency range for (a) PU/xGnP, (b) PU/EG, (c) PU/CB, and (d) PU/MWCNT with various filler contents.

nanotubes and interfacial surface areas throughout the composite able to interact with the incident radiation [6], which can significantly improve the SE.

Shielding is a result of different mechanisms such as reflection, (SE_R), absorption (SE_A), and multiple reflection [12]. To investigate the contribution of reflection and absorption to the total EMI SE of the composites, the incident (I), transmitted (T), and reflected (R) power data were collected directly by the instrument used to measure the EMI SE of the sample. The complex scattering parameters that represent the reflection S_{11} (S_{22}) and transmission S_{12} (S_{21}) coefficients are given by Eqs. 2 and 3 [20]:

$$T = \left| \frac{E_T}{E_I} \right|^2 = |S_{12}|^2 \left(= |S_{21}|^2 \right) \qquad (2)$$

$$R = \left| \frac{E_R}{E_I} \right|^2 = |S_{11}|^2 \left(= |S_{22}|^2 \right) \qquad (3)$$

The absorption power (A) is then determined by

$$A = 1 - R - T \qquad (4)$$

where R is the reflection power obtaining from S_{11} (S_{22}) scattering parameter, and T is the transmission power

obtaining from S_{21} (S_{12}) scattering parameter. In these measurements, it was considered that the incident power used in the experiments was 1 mW [13]. The contribution of SE_A (dB) and SE_R to the EMI SE of PU and composites was calculated according to Eqs. (5–7) [17, 20]:

$$SE_R = 10 \log \frac{I}{I-R} \qquad (5)$$

$$SE_A = 10 \log \frac{I-R}{T} \qquad (6)$$

$$EMI\ SE = SE_A + SE_R = 10 \log \frac{I}{I-R} + 10 \log \frac{I-R}{T}$$

$$= 10 \log \frac{I}{T} \qquad (7)$$

The contribution of reflection and absorption in the total EMI SE as average values in the frequency range from 8.2 to 12.4 GHz is reported in Fig. 6. It is possible to note that the shielding by reflection and absorption contribute to the total electromagnetic shielding and the contribution of both mechanism increases with the increasing of carbonaceous fillers loading, resulting in higher EMI SE. However, the main mechanism observed in the composites based on carbonaceous fillers is by absorption.
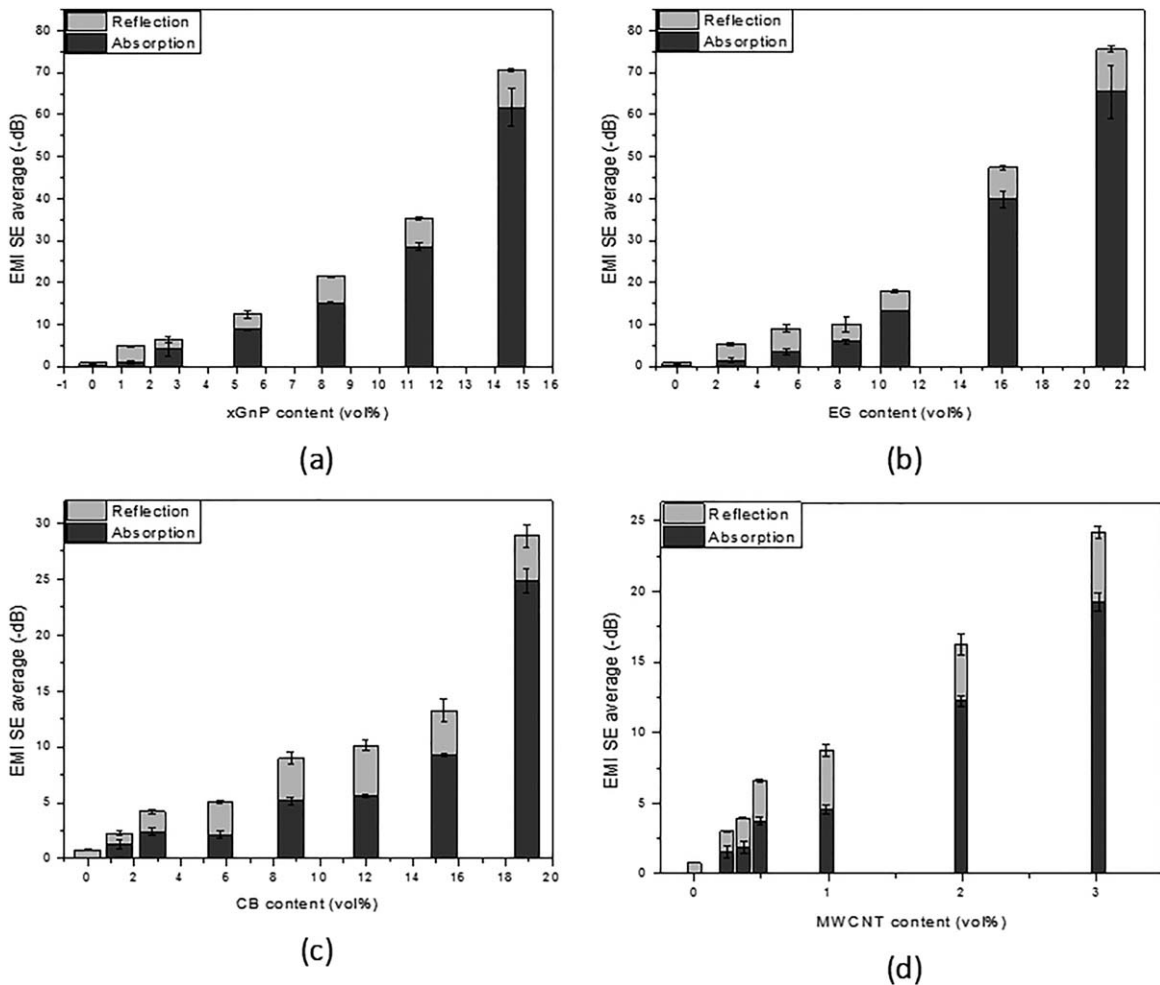
FIG. 6. Influence of absorption and reflection mechanisms on the EMI SE for (a) PU/xGnP, (b) PU/EG, (c) PU/CB, and (d) PU/MWCNT with various filler contents.

Table 3 shows the total SE, SE by reflection and absorption and electrical conductivity of neat PU and composites. It is worthwhile to note that the EMI SE of composites is strictly related to its electrical conductivity, as previously discussed. PU/EG exhibits the highest EMI SE and conductivity values when compared to the other systems, even higher filler content were used. However, if we take into account a given electrical conductivity level (example.g., $\times 10^{-1}$ S cm^{-1}) for composites containing different fillers, it possible to note that the EMI SE of the composites under investigation varies significantly. At the selected electrical conductivity, level EMI SE of PU/xGnP, PU/EG, PU/CB, and PU/MWCNT is -35, -47, -29, and -24 dB, respectively. The better EMI SE of PU/EG composites can be attributed to the plate-like morphology of graphite and the higher filler amount (16.1 vol%) presented in the composite that improve the interaction with the radiation and, consequently the EMI SE. According to Magioli, Soares, Sirqueira, Rahaman, and Khastgir [8], when the conductive network becomes denser, it can interact more efficiently with the incident electromagnetic radiation. These results confirm that EMI SE is not only dependent on electrical conductivity but also influenced by the morphology of filler, its amount, distribution, and dispersion level in the polymer matrix.

The EMI SE typically required for commercial application is about -20 dB [6, 18], which corresponds to <1% of transmitted electromagnetic wave. The results reported in this work indicate that by using 3 vol% of MWCNT into the PU matrix, it is possible to attain EMI SE levels superior than those required for commercial applications. However, it important to highlight that for the other systems based on xGnP and EG were also obtained more than 99.9% of attenuation, but the amount of the filler required to formulate a composite with this EMI SE level is significantly higher. An SE of -30 dB, corresponding to 99.9% of radiation attenuation is considered an elevated level for EMI SE applications [19]. The most efficient filler will depend on requirement of each specific application, taking cost and mechanicals properties into consideration.

TABLE 3. Total shielding effectiveness (EMI SE (dB and %)), shielding effectiveness by reflection (SE$_R$ (%)), shielding effectiveness by absorption (SE$_A$ (%)), and electrical conductivity (σ) of neat PU and composites.

System	Additive (vol%)	Additive (wt%)	SE$_A$ ($-$dB)	SE$_R$ ($-$dB)	EMI SE total ($-$dB)	EMI SE$_{Total}$ (%)	σ (S cm^{-1})
PU	0	0	0.07 ± 0.02	0.72 ± 0.02	0.79 ± 0.05	16.66	$(1.19 \pm 0.07) \times 10^{-15}$
PU/xGnP	1.3	2.5	1.12 ±0.35	3.78 ±0.17	4.90 ± 0.46	45.33	$(3.33 \pm 0.52) \times 10^{-14}$
	2.6	5.0	4.06 ± 1.71	2.23 ± 0.82	6.29 ± 2.75	73.26	$(1.69 \pm 0.12) \times 10^{-10}$
	5.4	10.0	8.79 ± 0.08	3.52 ± 0.81	12.31 ± 0.78	94.04	$(2.44 \pm 0.89) \times 10^{-6}$
	8.3	15.0	15.20 ± 0.13	6.29 ± 0.15	21.49 ± 0.11	99.29	$(9.24 \pm 0.03) \times 10^{-2}$
	11.4	**20.0**	**28.53 ± 0.81**	**6.79 ± 0.38**	**35.33 ± 0.5**	**99.97**	$\mathbf{(4.29 \pm 0.25) \times 10^{-1}}$
	14.6	25.0	61.71 ± 4.44	8.84 ± 0.37	70.56 ±4.37	99.99999	1.75 ± 0.01
PU/EG	2.7	5.0	1.48 ± 0.37	3.85 ± 0.36	5.33 ± 0.57	70.51	$(1.62 \pm 0.22) \times 10^{-14}$
	5.4	9.0	3.31 ±0.72	5.70 ± 0.77	9.10 ±0.56	87.41	$(1.06 \pm 0.41) \times 10^{-4}$
	8.3	13.0	5.91 ± 0.47	4.00 ± 1.78	9.91 ± 2.21	88.45	$(7.56 \pm 0.02) \times 10^{-3}$
	10.7	17.0	13. 26 ± 0.10	4.62 ± 0.24	17.88 ± 0.32	98.37	$(7.64 \pm 0.33) \times 10^{-2}$
	16.1	**25.0**	**39.83 ± 1.94**	**7.58 ± 0.51**	**47.41 ± 1.45**	**99.99808**	$\mathbf{(8.12 \pm 0.20) \times 10^{-1}}$
	21.4	32.0	65.40 ± 631	10.20 ± 0.64	75.61 ± 6.33	99.99999	3.78 ± 0.09
PU/CB	1.4	2.5	1.31 ± 0.39	0.95 ± 0.19	2.26 ± 0.32	40.44	$(2.46 \pm 0.27) \times 10^{-15}$
	2.8	5.0	2.42 ± 0.37	1.78 ± 0.22	4.20 ± 0.31	61.89	$(3.31 \pm 0.68) \times 10^{-14}$
	5.7	10.0	2.12 ± 0.32	2.93 ± 0.12	5.05 ± 0.41	68.67	$(3.43 \pm 0.13) \times 10^{-11}$
	8.8	15.0	5.14 ± 0.35	3.83 ± 0.56	8.98 ± 0.29	87.34	$(3.19 \pm 0.03) \times 10^{-7}$
	12.0	20.0	5.60 ± 0.19	4.52 ± 0.50	10.13 ± 0.41	90.26	$(8.36 \pm 0.91) \times 10^{-7}$
	15.4	25.0	9.22 ± 0.14	4.01 ± 1.02	13.24 ± 0.99	95.15	$(1.65 \pm 0.24) \times 10^{-2}$
	18.9	**30.0**	**24.02 ± 1.05**	**4.85 ± 1.08**	**28.87 ± 0.16**	**99.74**	$\mathbf{(2.10 \pm 0.04) \times 10^{-1}}$
PUAIWCNT	0.2	0.5	1.54 ± 0.41	1.45 ± 0.08	2.99 ± 0.38	49.66	$(2.80 \pm 0.87) \times 10^{-14}$
	0.4	0.75	1.87 ± 0.37	2.07 ± 0.06	3.95 ± 0.41	59.57	$(1.90 \pm 0.62) \times 10^{-10}$
	0.5	1.0	3.72 ± 0.27	2.85 ± 0.13	6.57 ± 0.36	77.92	$(1.40 \pm 0.12) \times 10^{-9}$
	1.0	2.0	4.55 ± 027	4.19 ± 0.42	8.74 ± 0.68	86.51	$(1.50 \pm 0.44) \times 10^{-7}$
	2.0	4.0	12.25 ± 038	3.96 ± 0.74	16.22 ± 0.45	97.60	$(5.10 \pm 0.08) \times 10^{-3}$
	3.0	**6.0**	**19. 26 ± 0.62**	**4.88 ± 0.44**	**24.14 ± 0.27**	**99.61**	$\mathbf{(1.90 \pm 0.27) \times 10^{-1}}$

Table 4 presents the EMI SE for some polymer composites containing carbonaceous fillers reported in the open scientific literature. It is interesting to note that the carbonaceous/PU composites produced in this work manifest EMI SE significantly higher than other composites containing xGnP and EG, and lower values than those reported for composites filled with CB. The level of shielding of PU/MWCNT is quite similar to those previously reported in the literature for other polymeric matrices.

TABLE 4. EMI SE values for some composites filled with carbonaceous fillers reported in the literature.

		EMI SE ($-$dB)/filler				
Matrix	Filler content vol% (wt%)	xGnP	EG	CB	CNT	Reference
Epoxy	8.8 (15)	21	—	—	—	14
TPU	5.3 (10)	—	—	12.2	21.8	17
SEBS	8.2 (15)	—	—	17.56	—	13
SEBS	11.2 (20)	—	11.69	—	—	13
ABS	8.2 (15)	—	—	20	—	18
ABS	2.6 (5)	—	—	—	30	18
PS	0.5 (1)	—	—	—	7.6–8.5	6
PTT	5.3 (10)	—	—	—	36–42	7
PU	11.2 (20)	—	—	—	16–17	5

CONCLUSIONS

Composites based on thermosetting polyurethane (PU) derived from castor oil filled with various amount of graphene nanoplatelets, expanded graphite, carbon black, and MWCNTs were developed. The results reported in this work demonstrate that by using different carbonaceous fillers, it is possible to achieve various levels of EMI SE at different filler loading. The use of low conductive additives content can be beneficial to preserve the physical properties of matrix and reduce the cost. Based on the electrical conductivity obtained for the systems investigated in this work, we can conclude that the use of MWCNT is more advantageous, as at low loading (3 vol%), it is possible to reach a maximum electrical conductivity of 0.19 S cm^{-1}, which is quite similar to that found for neat MWCNTs. At the same loading, the xGnP-, EG-, and CB-based composites are not conductive. For composites containing a given carbon filler, the EMI SE increases with increasing the filler content. On the other hand, EMI SE values for composites are influenced by the filler type used. This behavior indicates that EMI SE is also dependent on the morphology, aspect ratio, and dispersion of fillers. Composite based on PU/EG and PU/xGnP exhibited the highest EMI SE values, reaching values of -76 and -70 dB at filler loading of 21.4 and 14.6 vol%, respectively, which is corresponding

to 99.999% of radiation attenuation. The good performance of these composites can be attributed to the plate-like morphology that display elevated aspect ratio and it is able to form a denser network, which interact more efficiently with the incident electromagnetic radiation. However, composites based on PU/MWCNT displays the highest EMI level at the lower filler content due to the higher aspect ratio of MWCNT which facilitates the formation of a conductive network, contributing with the electromagnetic radiation interaction. CB appears to be the less efficient filler due to the poor distribution into the PU matrix, which results in regions transparent to magnetic waves. Furthermore, the main mechanism of attenuation is based on absorption, which become these composites an interesting alternative to replace reflective metallic materials.

ACKNOWLEDGMENTS

REFERENCES

1. J.-M. Thomassin, C. Jérôme, T. Pardoen, C. Bailly, I. Huynen, and C. Detrembleur, *Mat. Sci. Eng.*, **74**, 211 (2013).

2. D.D.L. Chung, *Carbon*, **39**, 279 (2001).

3. M. Rahaman, T.K. Chaki, and D. Khastgir, *J. Mater. Sci.*, **46**, 3989 (2011).

4. Y. Wang and X. Jing, *Polym. Adv. Technol.*, **16**, 344 (2005).

5. Z. Liu, G. Bai, Y. Huang, Y. Ma, F. Du, F. Li, T. Guo, and Y. Chen, *Carbon*, **45**, 821 (2007).

6. Y. Yang, M.C. Gupta, and K.L. Dudley, *Nanotechnology*, **18**, 345701 (2007).

7. A. Gupta and V. Choudhary, *Compos. Sci. Technol.*, **71**, 1563 (2011).

8. M. Magioli, B.G. Soares, A.S. Sirqueira, M. Rahaman, and D. Khastgir, *J. Appl. Polym. Sci.*, **125**, 1476 (2012).

9. J. Huo, L. Wang, and H. Yu, *J. Mater. Sci.*, **44**, 3917 (2009).

10. J.S.F. Barrett, A.A. Abdala, and F. Srienc, *Macromolecules*, **47**, 3926 (2014).

11. S. Stankovich, D.A. Dikin, G.H.B. Dommett, K.M. Kohlhaas, E.J. Zimney, E.A. Stach, R.D. Piner, S.T. Nguyen, and R.S. Ruoff, *Nature*, **442**, 282 (2006).

12. Y. Bingqing, Y. Liming, S. Leimei, A. Kang, and Z. Xinluo, *J. Phys. D Appl. Phys.*, **45**, 235108 (2012).

13. S. Kuester, C. Merlini, G.M.O. Barra, J.C. Ferreira, Jr, A. Lucas, A.C. de Souza, and B.G. Soares, *Compos. B Eng.*, **84**, 236 (2016).

14. J. Liang, Y. Wang, Y. Huang, Y. Ma, Z. Liu, J. Cai, C. Zhang, H. Gao, and Y. Chen, *Carbon*, **47**, 922 (2009).

15. A. Aqel, K.M.M.A. El-Nour, R.A.A. Ammar, and A. Al-Warthan, *Arab. J. Chem.*, **5**, 1 (2012).

16. T. Belin and F. Epron, *Mat. Sci. Eng. B*, **119**, 105 (2005).

17. S.D.A.S. Ramôa, G.M.O. Barra, R.V.B. Oliveira, M.G. de Oliveira, M. Cossa, and B.G. Soares, *Polym. Intern.*, **62**, 1477 (2013).

18. M.H. Al-Saleh, W.H. Saadeh, and U. Sundararaj, *Carbon*, **60**, 146 (2013).

19. M.H. Al-Saleh and U. Sundararaj, *Carbon*, **47**, 1738 (2009).

20. C. Merlini, G.M.O. Barra, M.D.P.P. da Cunha, S.D.A.S. Ramôa, B.G. Soares, and A. Pegoretti, *Polym. Compos.* in press.

21. M. Bevilacqua, C. Bianchini, A. Marchionni, J. Filippi, A. Lavacchi, H. Miller, W. Oberhauser, F. Vizza, G. Granozzi, L. Artiglia, S.P. Annen, F. Krumeich, and H. Grutzmacher, *Energ. Environ. Sci.*, **5**, 8608 (2012).

22. M. Traina, A. Pegoretti, and A. Penati, *J. Appl. Polym. Sci.*, **106**, 2065 (2007).

23. C. Merlini, S.D.A.S. Ramôa, and G.M.O. Barra, *Polym. Compos.*, **34**, 537 (2013).

24. E. Thostenson, C. Li, and T. Chou, *Compos. Sci. Technol.*, **65**, 491 (2005).

25. S.D.A.S. Ramoa, G.M.O. Barra, C. Merlini, S. Livi, B.G. Soares, and A. Pegoretti, *Exp. Polym. Lett.*, **9**, 945 (2015).

26. B. Wessling and B. *Polym. Eng. Sci.*, **31**, 1200 (1991).